Electronic Supplementary Information

Ultrathin Al Foils to Fabricate Dendrite-Free Li-Al Anodes

Lan Wu, Guang He*, Yi Ding*

Tianjin Key Laboratory of Advanced Functional Porous Materials, Institute for New Energy Materials and Low-Carbon Technologies, School of Materials Science and Engineering, Tianjin University of Technology, Tianjin, 300384, P. R. China

E-mail: yding@tjut.edu.cn, heguang@tjut.edu.cn

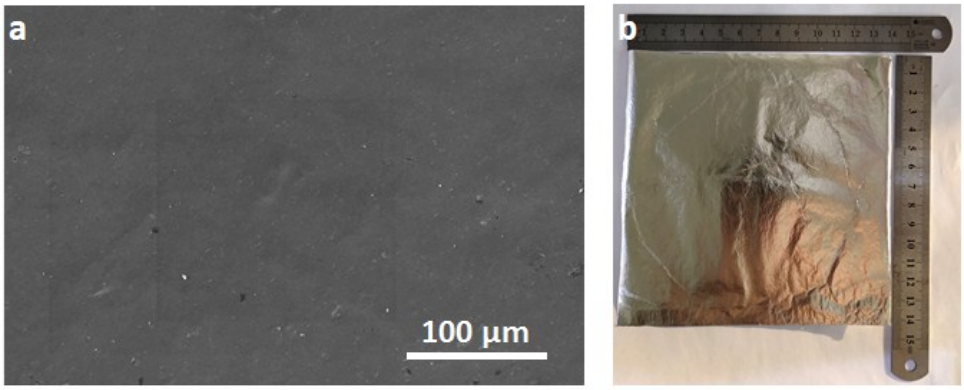

Figure S1. (a) The SEM and (b) optical images of the ultrathin Al foil.

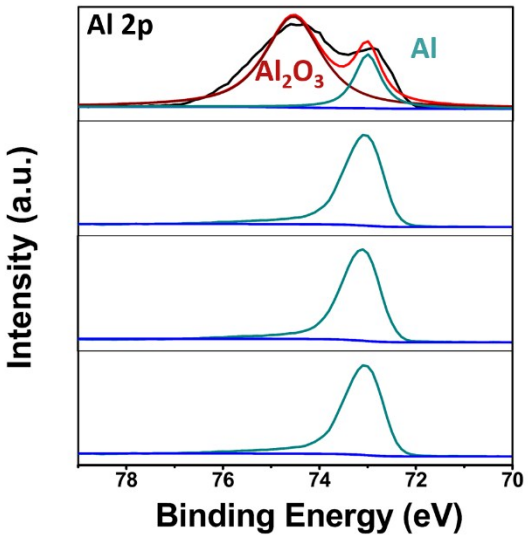

Figure S2. XPS spectra of the Al-UTF showing the Al 2p regions upon Ar sputtering for 0 sec, 30 secs, 60 secs and 90 secs, respectively.

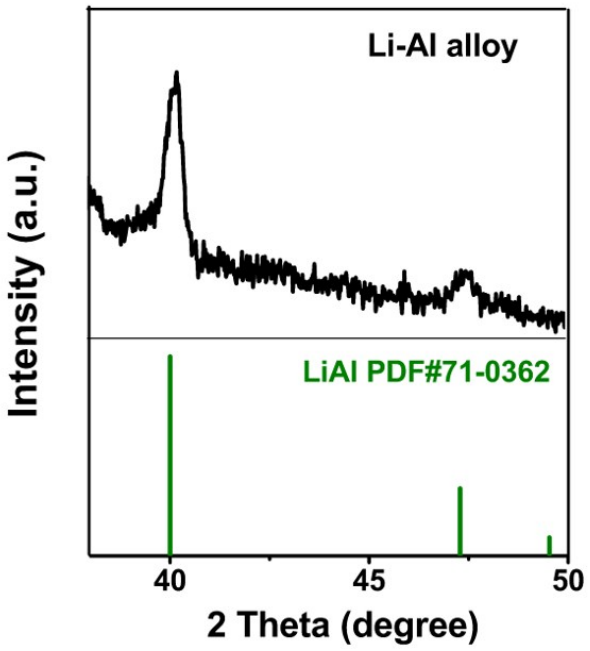

Figure S3. The XRD pattern with magnified regions of the LAL composite anode.

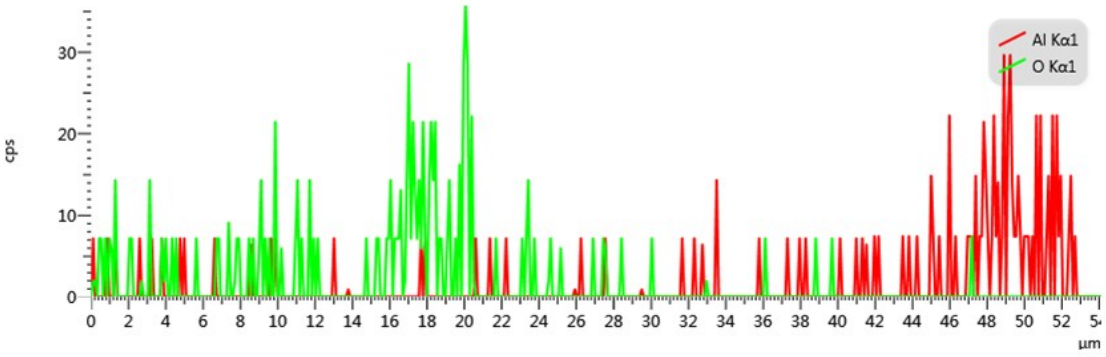

Figure S4. The overall elemental analysis of the LAL composite anode.

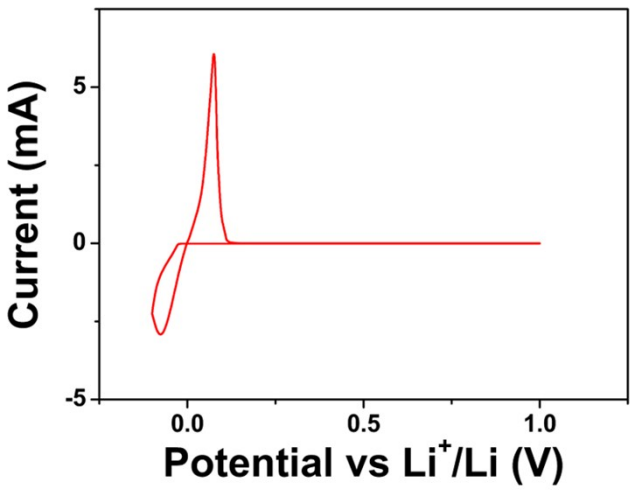

Figure S5. The cyclic voltammetry (CV) curve of Li plating onto Cu foil.

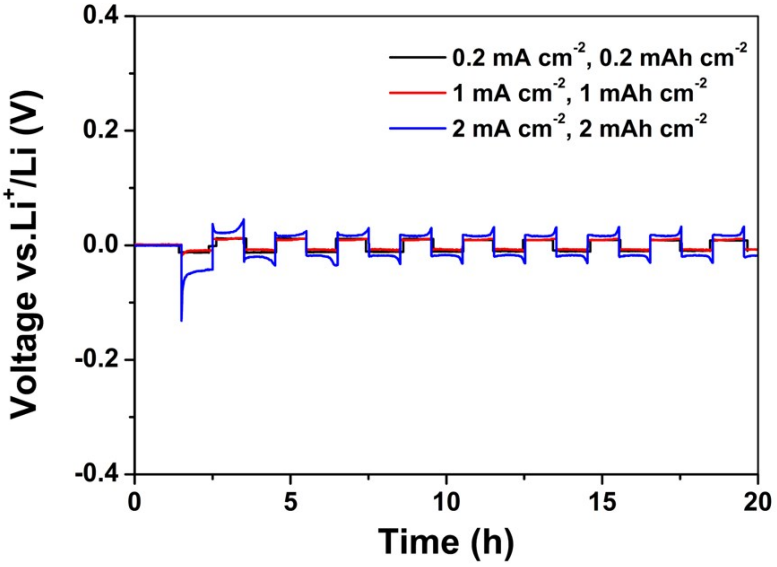

Figure S6. Voltage profiles with plating/stripping capacities of LAL|LAL of 0.2 mAh cm^{-2} at 0.2 mA cm^{-2}, 1 mAh cm^{-2} at 1 mA cm^{-2} and 2 mAh cm^{-2} at 2 mA cm^{-2}.

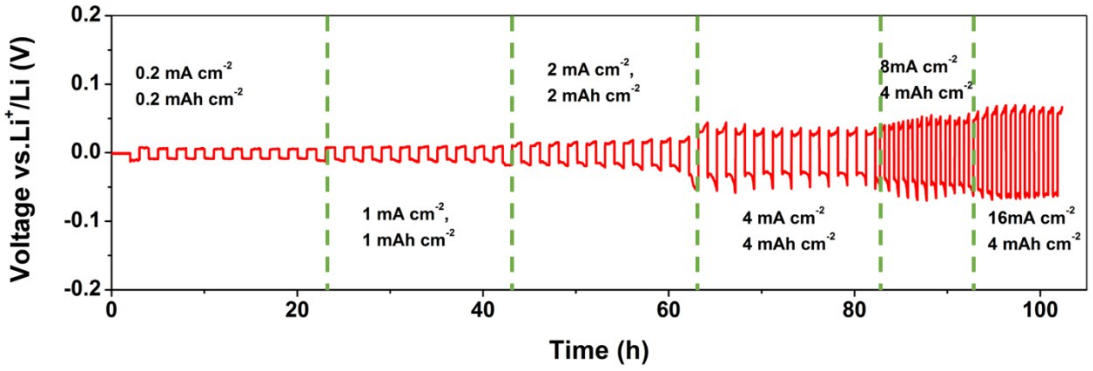

Figure S7. The rate performance of LAL|LAL symmetrical cell.

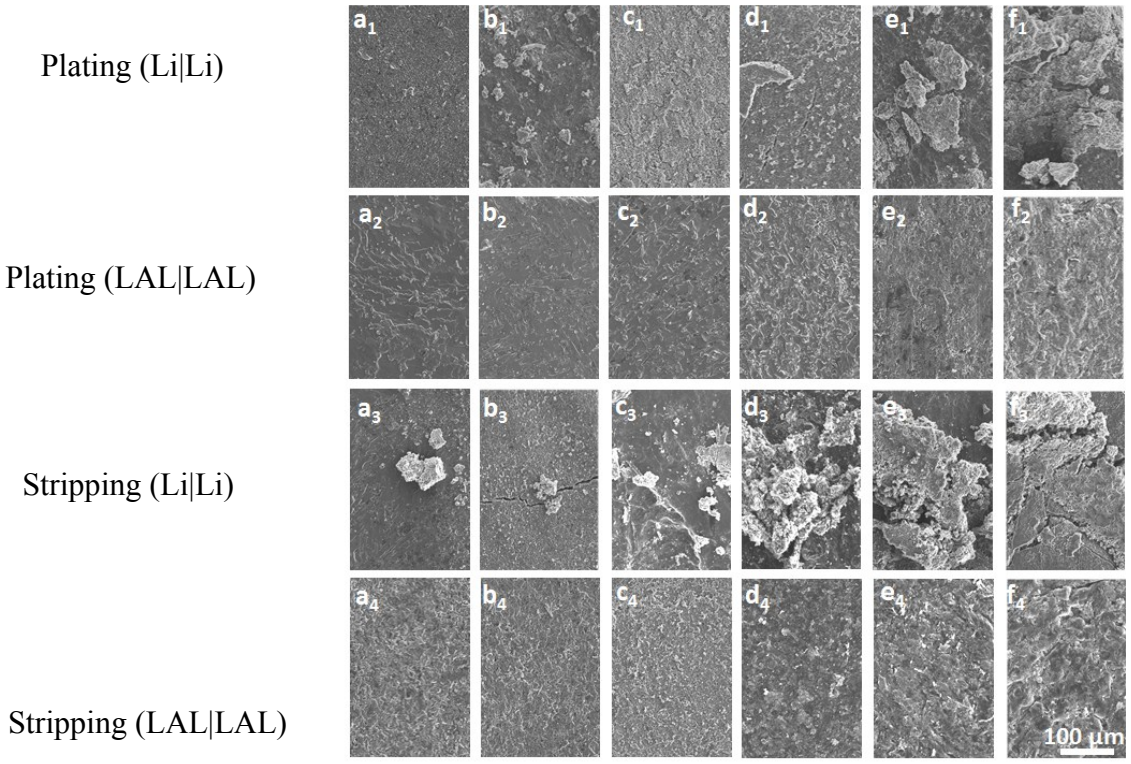

Figure S8. The top-view SEM images of pure lithium foil and LAL alloy after 10 cycles in different currents. (a) 0.2 mA cm^{-2}, 0.2 mAh cm^{-2},(b) 1 mA cm^{-2}, 1 mAh cm^{-2}, (c) 2 mA cm^{-2}, 2 mAh cm^{-2}, (d) 4 mA cm^{-2}, 4 mAh cm^{-2}, (e) 8 mA cm^{-2}, 4 mAh cm^{-2}, (f) 16 mA cm^{-2}, 4 mAh cm^{-2}. And 1 and 3 are pure lithium foils at the state of plating and stripping, respectively. 2 and 4 corresponds to the LAL anodes.

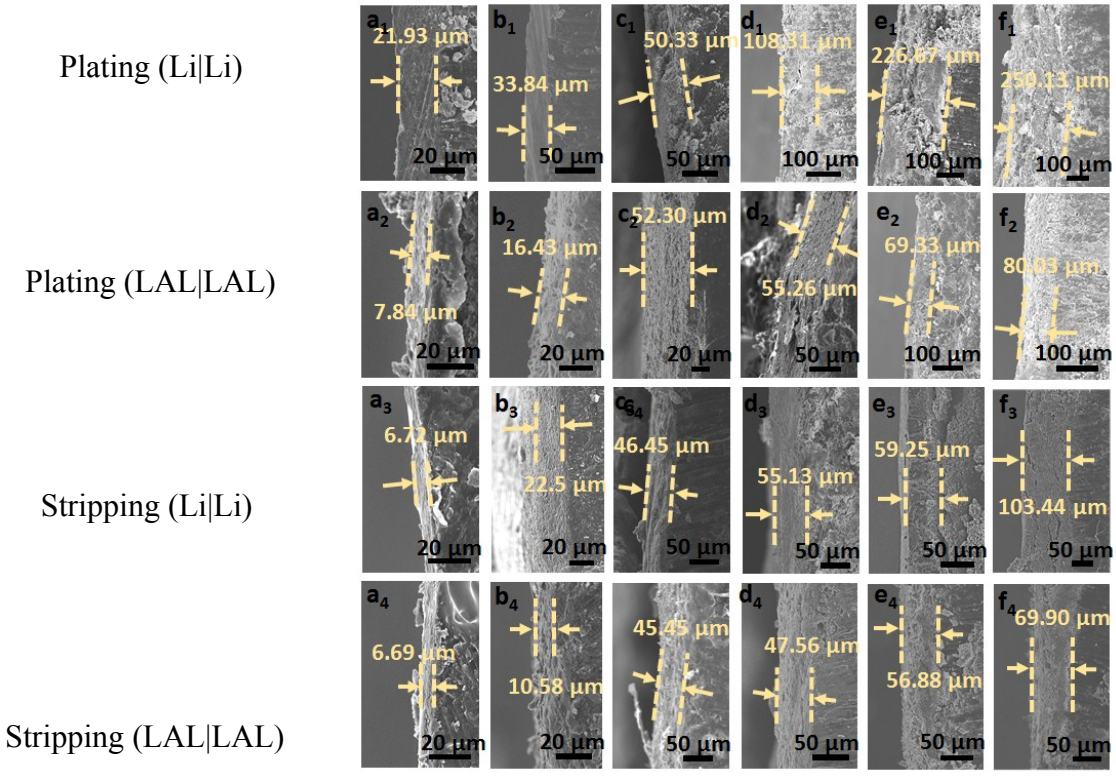

Figure S9. The cross-sectional SEM images of pristine Li anodes and LAL composite anodes after 10 cycles in different current densities and capacities in symmetrical cells. (a) 0.2 mA cm^{-2}, 0.2 mAh cm^{-2}, (b) 1 mA cm^{-2}, 1 mAh cm^{-2}, (c) 2 mA cm^{-2}, 2 mAh cm^{-2}, (d) 4 mA cm^{-2}, 4 mAh cm^{-2}, (e) 8 mA cm^{-2}, 4 mAh cm^{-2}, (f) 16 mA cm^{-2}, 4 mAh cm^{-2}. In each image, 1 and 3 are pristine lithium anodes after plating and stripping, while 2 and 4 correspond to LAL composite anodes after plating and stripping, respectively.

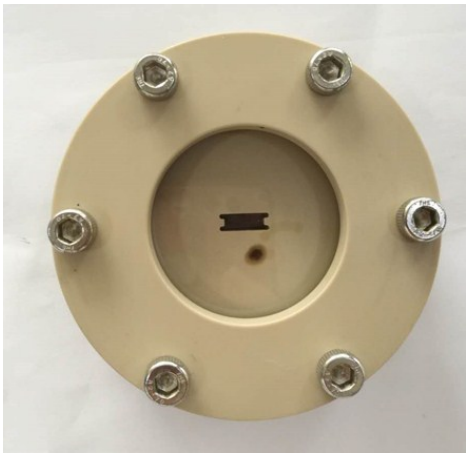

Figure S10. The optical image of the in-situ cell.

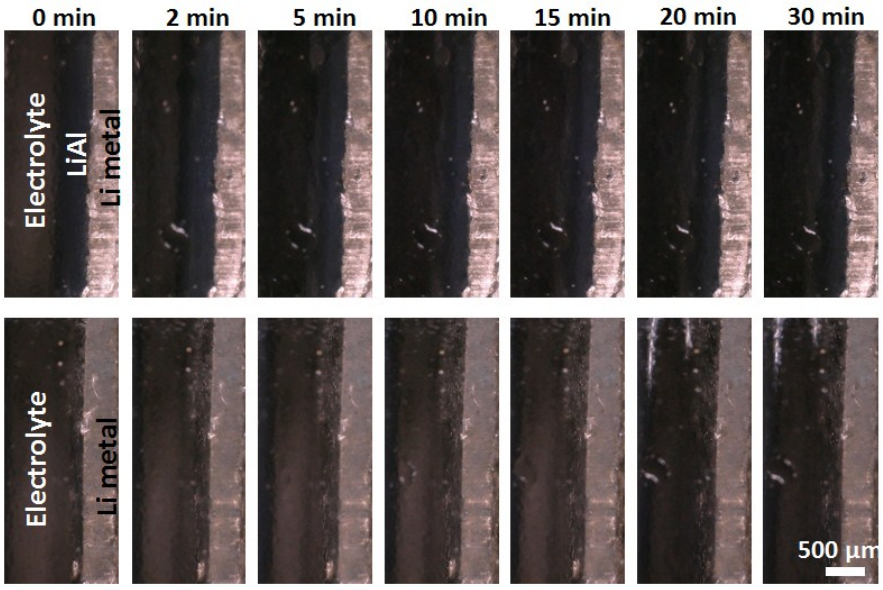

Figure S11. The optical microscopy images of the electrolyte/electrode interface as a function of time at 0.2 mA cm^{-2}.

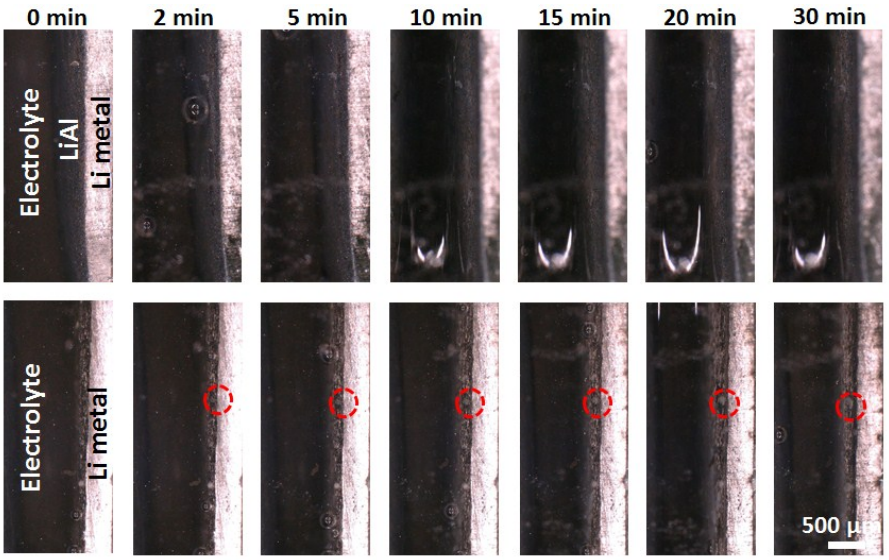

Figure S12. The optical microscopy images of the electrolyte/electrode interface as a function of time at 1 mA cm^{-2}.

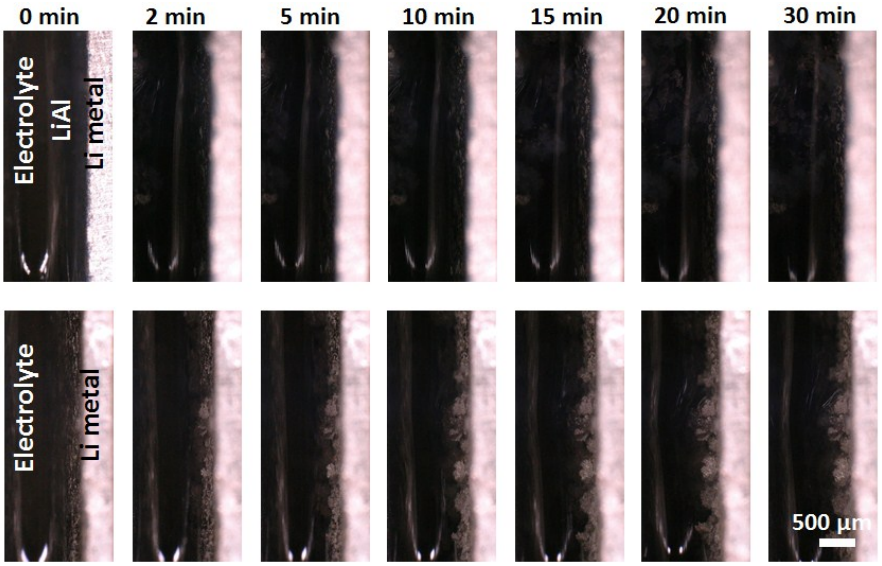

Figure S13. The optical microscopy images of the electrolyte/electrode interface as a function of time at 2 mA cm^{-2}.

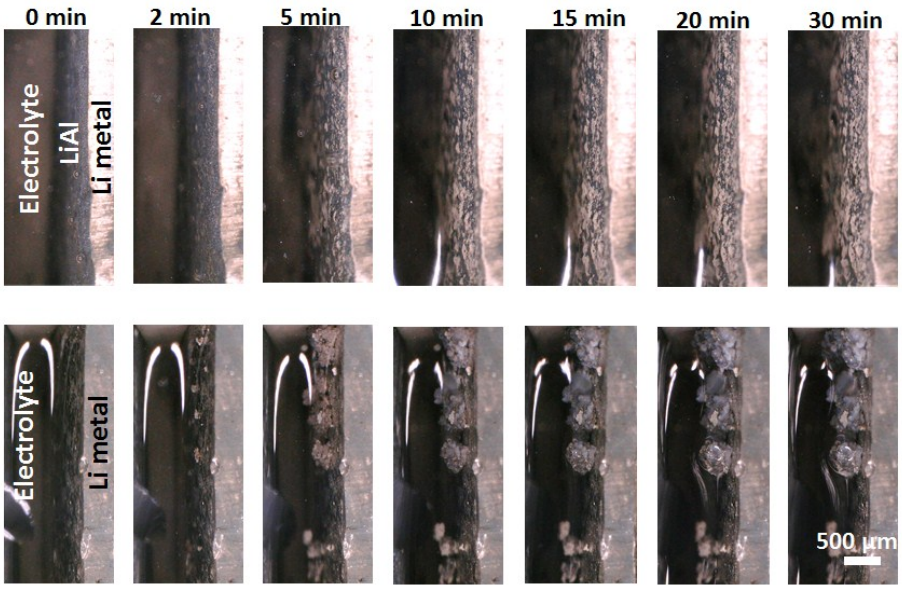

Figure S14. The optical microscopy images of the electrolyte/electrode interface as a function of time at 4 mA cm^{-2}.

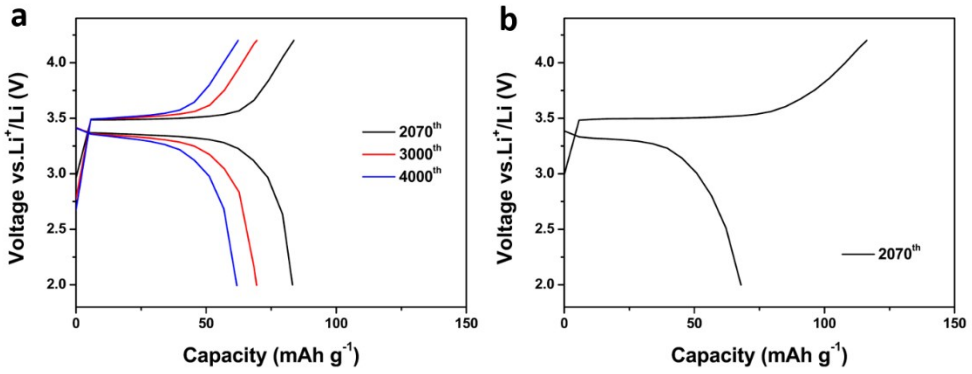

Figure S15. Charge/discharge profiles of cells assembled with (a) LAL and (b) pristine Li anodes using LFP cathodes at 2C.

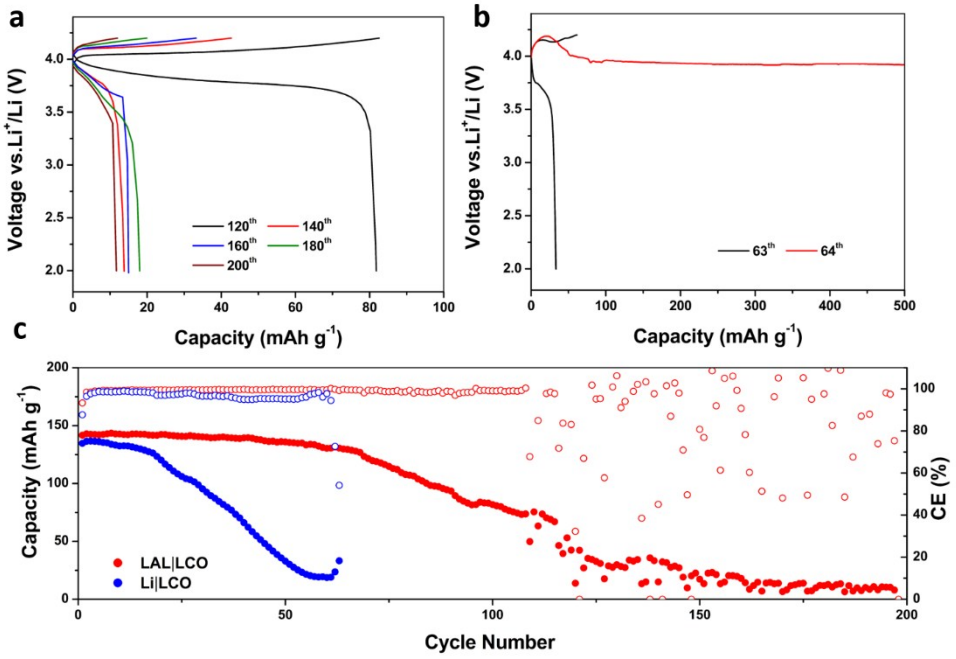

Figure S16. Charge/discharge profiles of (a) LAL|LCO and (b) Li|LCO cells, and (c) long-term cycling performance of the cells.

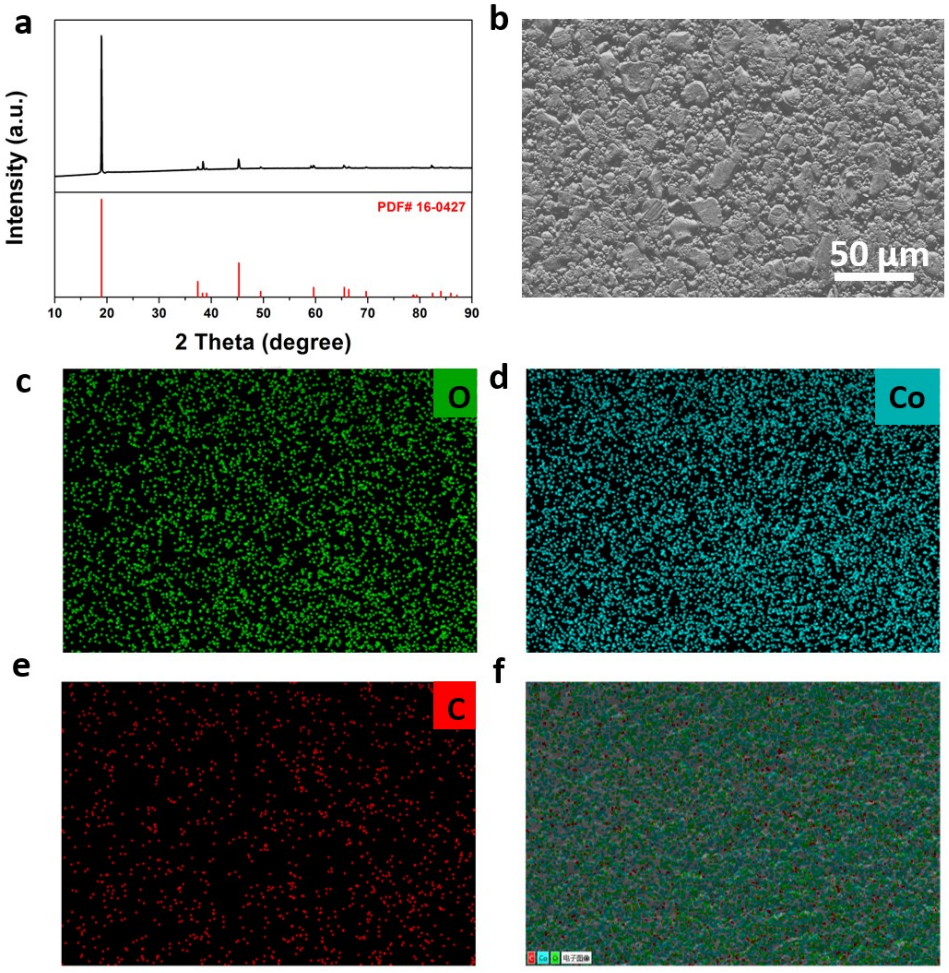

Figure S17. (a) The XRD pattern of LCO electrode. (b) The SEM image of LCO cathode and (c-e) the corresponding elemental maps of O, Co and C. (f) The elemental mapping image of mixed O, Co and C.

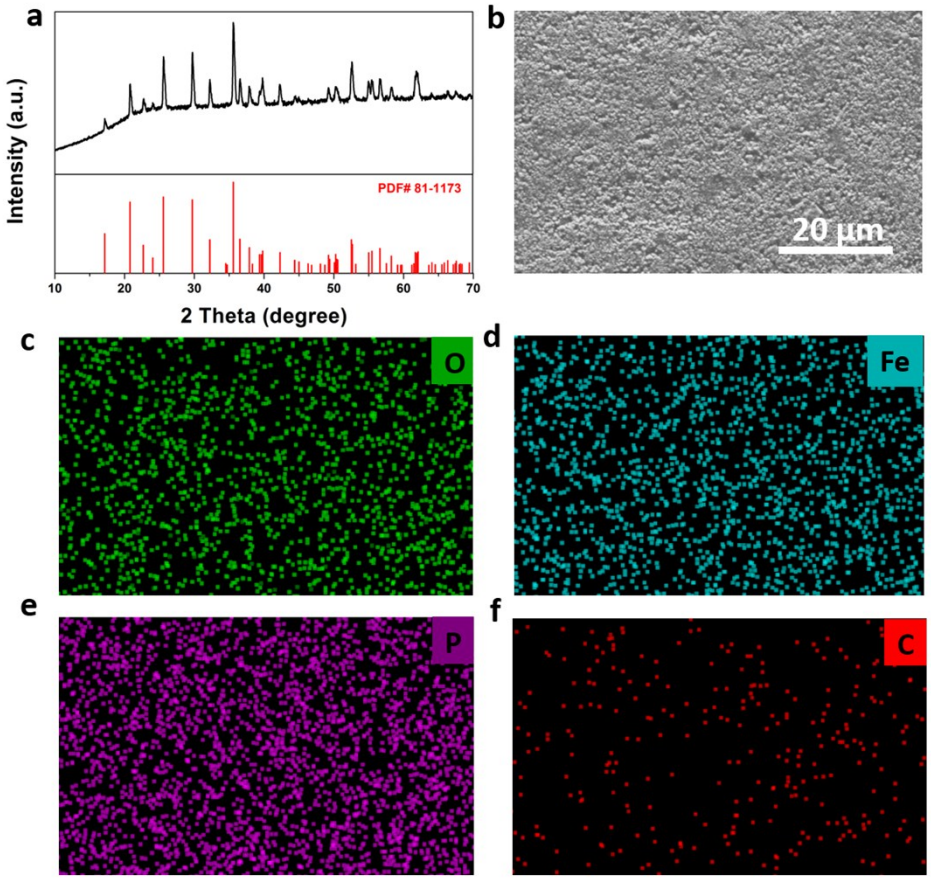

Figure S18. (a) The XRD pattern of LFP electrode. (b) The SEM image of LFP cathode. (c)-(f) The elemental maps of O, Fe, P and C, where the atomic ratios of P:Fe:O are 0.23:0.25:1, very close to the formula unit of $LiFePO_4$.

Table S1. The performance comparison of lithium metal batteries using lithium-metal alloy anodes.

	Protection methods	Preparation methods	Working electrodes	Overpotential	Cycling life	High-rate performance
This work	**Li-Al anodes (ultrathin Al foil)**	**Physical integration**	**LAL|LAL**	**~25 mV at 0.2 m A cm^{-2}; ~100 mV at 2 mA cm^{-2}**	**0.2 mA cm^{-2}, 1h, 7000h; 2 mA cm^{-2}, 1 h, 600h**	**8 mA cm^{-2}, 0.5 h, 400h**
Ref. S1	$Li_{13}In_3$ alloy	Chemical surface modification	$Li_{13}In_3$|Li	~200 mV at 2 mA cm^{-2}	2 mA cm^{-2},1 h, >1200 h	2 mA cm^{-2},1 h, >1200 h
Ref. S2	Li-Sn alloy	Chemical surface modification	Li-Sn|Li-Sn	~450 mV at 3 mA cm^{-2}	3 mA cm^{-2}, 1 h, 500 h	3 mA cm^{-2}, 1 h, 500 h
Ref. S3	Li_xSi alloy	Sputtering and heating	Li|Li-Li_xSi	~40 mV at 1 mA cm^{-2}	1 mA cm^{-2}, 1 h, 400 h	1 mA cm^{-2}, 1 h, 400 h
Ref. S4	Li_xSn	Roll-to-roll prelithiation	LixSn|LFP	-	2.28 mAh cm^{-2}	-
Ref. S5	LiAl alloy	Magnetron sputtering treatment on porous 3D Cu	3D Cu@Al@Li|3 D Cu@Al@Li	~50 mV at 0.5 mA cm^{-2}	0.5 mA cm^{-2}, 2 h, 1700 h	1 mA cm^{-2}, 1 h, <1500 h
Ref. S6	Li-In	Machine-press	Li-In| Li-In	~50 mV at 0.5 mA cm^{-2}	0.5 mA cm^{-2}, 1 h, 585 h	1 mA cm^{-2}, 3 h, <500 h
Ref. S7	Cu-Al@Al	Physical vapor deposition	Cu-Al@Al|Li	-	2 mA cm^{-2}, 0.5 h, <200 h	2 mA cm^{-2}, 0.5 h, <200 h
Ref. S8	3D porous Cu	Pressed with punching machine	3D Cu/Li|3D Cu/Li	~100 mV at 0.5 mA cm^{-2}	0.5 mA cm^{-2}, 2 h, 1280 h	2 mA cm^{-2}, 0.5 h, 120 h
Ref. S9	Carbon fiber-based composite	Electroplating Ag and molten Li	CF/Ag-Li|Li	~100 mV at 1 mA cm^{-2}	1 mA cm^{-2},1 h, 400 h	1 mA cm^{-2},1 h 400 h
Ref. S10	Surface-patterned lithium	Micro-fabrication techniques	spLi|spLi	~20 mV at 0.117 mA cm^{-2}	0.117 mA cm^{-2}, 2 h, 800 h	0.117 mA cm^{-2}, 2 h, 800 h
Ref S11	Vertically aligned CuO on Cu foil	Wet chemical reaction	Li|Li-(VA-CuO-Cu)	~30 mV at 0.5 mA cm^{-2}	0.2 mA cm^{-2},1 h, 1500 h	0.5 mA cm^{-2},1 h, 700 h
Ref. S12	Nitrogen-doping carbon foam	Carbonization	NGCF@Li |NGCF@Li	30 mV at 2 mA cm^{-2}	2 mA cm^{-2},0.5 h, 1200 h	3 mA cm^{-2},1/3 h, <650 h
Ref. S13	$AuLi_3$ particles	Electrodepositi-on of gold on Ni foam	Li|Li@($AuLi_3$ @Ni foam)	~20 mV at 0.117 mA cm^{-2}	0.5 mA cm^{-2}, 2 h, 740 h	0.5 mA cm^{-2}, 2 h, 740 h
Ref. S14	GF-LiF-Li	Graphite fluoride reacts with molten Li	GF-LiF-Li|GF-LiF-Li	~200 mV at 1 mA cm^{-2}	1 mA cm^{-2}, 1 h, <250 h	10 mA cm^{-2}, 0.1 h, 33.3 h

References

[1] X. Liang, Q. Pang, I. R. Kochetkov, M. S. Sempere, H. Huang, X, Sun, L. F. Nazar, *Nat. Energy* 2017, **2**,17119.

[2] Z. Tu, S. Choudhury, M. J. Zachman, S. Wei, K. Zhang, L. F. Kourkoutis, L. A. Archer, *Nat. Energy* 2018, **3**, 310.

[3] W. Tang, X. Yin, S. Kang, Z. Chen, B. Tian, S. L. Teo, X. Wang, X. Chi, K. P. Loh, H. Lee, G. W. Zheng, *Adv. Mater.* 2018, **30**, 1801745.

[4] H. Xu, S. Li, C. Zhang, X. Chen, W. Liu, Y. Zheng, Y. Huang, J. Li, *Energy Environ. Sci.* 2019, DOI: 10.1039/C9EE01404G.

[5] H. Ye, Z. Zheng, H. Yao, S. Liu, T. Zuo, X. Wu, Y. Yin, N. Li, J. Gu, F. Cao, Y. Guo, *Angew. Chem. Int. Ed.* 2019, **58**, 1094.

[6] B. Sun, J. Lang, K. Liu, N. Hussain, M. Fang, H. Wu, *Chem. Commun.* 2019, **55**, 1592.

[7] M. Zhang, L. Xiang, M. Galluzzi, C. Jiang, S. Zhang, J. Li, Y. Tang, *Adv. Mater.* 2019, **31**, 1900826.

[8] Q. Li, S. Zhu, Y. Lu, *Adv. Funct. Mater.* 2017, **27**, 1606422.

[9] R. Zhang, X. Chen, X. Shen, X. -Q. Zhang, X. -R. Chen, X.-B. Cheng, C. Yan, C.-Z. Zhao, Q. Zhang, *Joule* 2018, **2**, 764.

[10] Q. Li, B. Quan, W. Li, J. Lu, J. Zheng, X. Yu, J. Li, H. Li, *Nano Energy*. 2018, **45**, 463.

[11] C. Zhang, W. Lv, G. Zhou, Z. Huang, Y. Zhang, R. Lyu, H. Wu, Q. Yun, F. Kang, Q.-H, Yang, *Adv. Energy Mater.* 2018, **8**, 1703404.

[12] L. Liu, Y.-X. Yin, J.-Y. Li, S.-H. Wang, Y.-G. Guo, L.-J. Wan, *Adv. Mater.* 2018, **30**, 1706216.

[13] X. Ke, Y. Liang, L. Ou, H. Liu, Y. Chen, W. Wu. Y. Cheng, Z. Guo, Y. Lai, P. Liu, Z. Shi, *Energy Storage Mater.* 2019, DOI: 10.1016/j.ensm.2019.04.003.

[14] X. Shen, Y. Li, T. Qian, J. Liu, J. Zhou, C. Yan, J. B. Goodenough, *Nat. Commun.* 2019, **10**, 900.